

Impact of faults on landslide in the Atharamura Hill (along the NH 44), Tripura

Subhajit Sen · Saptarshi Mitra · Chandrani Debbarma · Sunil Kumar De

Received: 6 March 2014 / Accepted: 5 October 2014 / Published online: 17 October 2014
© Springer-Verlag Berlin Heidelberg 2014

Abstract The present study is aimed at assessing the relationship between existing faults and occurrence of landslides. The geophysical techniques like geothermal imaging of fault zone, soil electrical resistivity data and field verification identify the fault characteristic. The present study reveals two prominent faults in the Atharamura Hill, i.e., one north–south extended faults, and the other east–west extended faults. The change in the geothermal characteristic along the fault, structural data (dip, strike) and most significantly the locations of landslide close to faults provide strong correlation of the landslide and the existing faults. The soil electrical resistivity data are low along the faults. The subsurface resistivity profile clearly delineates the faults.

Keywords Soil electrical resistivity · Debris fall · Rock slide · Earth fall · Strike slip fault

Introduction

Tectonically northeast India remained dynamic due to Indian Plate movements during the Tertiary and the Quaternary periods. Early works of Smith et al. (1970); McKenzie et al. (1971); Falvey (1974); Curry et al. (1974), (1982); Lee et al. (1995); Steacy et al. (1996); Varga (1997); Acharyya (1998) show the influence of plate

motion on landform evolution and depositional environmental changes in the study area. Geologically this area is characterized by early marine-coastal and estuarine depositions which strongly support that during the Miocene time the area was under marine environmental condition (Dey 2005). At present the study area is considered as one of the most active seismo-tectonic zones of the world (Gupta et al. 1982, 1986, 1989; Gupta 1993; Guha et al. 1984; Kayal 1987; Bhattacharjee 1998). According to the Bureau of Indian Standard's (BIS), Seismic hazard map of India (2000), the study area (Fig. 2a) falls within the Zone V (Jaisawal K and Sinha 2006). In some recent works on the Tripura fold belt (Dey et al. 2009, 2011a, b) several fault lines have been identified in the Baramura Hill and Gojalia fold which directly or indirectly play a significant role in the occurrence of hazards. Several methodological approaches have been used for identification of the fault. The present work is the continuation of that work. The Atharamura Hill is located in the eastern portion of the Baramura Hill. This hill range attracted the attention of the present researchers because of its unexplored geological mystery. Details of structural data on Atharamura Hill are not found. Some faults which play a key role in the occurrence of landslides in this hilly tract have been identified. Several methodological approaches were taken by early research to identify and eradicate landslide hazard in the hilly terrain (Eeckhaut et al. 2005, 2006; Sass et al. 2008; Booth et al. 2009).

It is observed that landslides in the hilly tract of Tripura State (India) are located in some of the specific areas. Considering the importance of landslide studies in north-east India it was decided to perform a study on landslide in a tectonically significant area of Tripura with the objective to identify the relationship between existing faults and landslides along the road side.

S. Sen · S. Mitra · C. Debbarma
Department of Geography and Disaster Management, Tripura University, Suryamaninagar 799022, India

S. K. De (✉)
Department of Geography, North Eastern Hill University,
Shillong 793022, India
e-mail: desunil@yahoo.com

Table 1 Stratigraphic detail of the study area (extracted from Lal et al. 2012) indicated that the Atharamura Hill comprises of Tipam and Surma Group

Age	Group	Formation	Member	Thickness (m)	Tectonic history
Recent		–	Alluvium	–	–
Pleistocene		Dihing		100–300	–
		Dupitila	Upper	200–400	
			Lower		
	Tipam	Girujan Clay	–	100–200	–
		Tipam Sandstone		1,500 (+)	
Miocene	Surma	Bokabil	–	1,500	Uplift Himalayas
		Bhuban	Upper	1,025	Major Himalayan Orogeny
			Middle	1,230	
			Lower	2,000 (+)	Subduction/ Folding Indo-Burma
Oligocene	Barail	Not penetrated			Early collision India–Eurasia Tethys closing

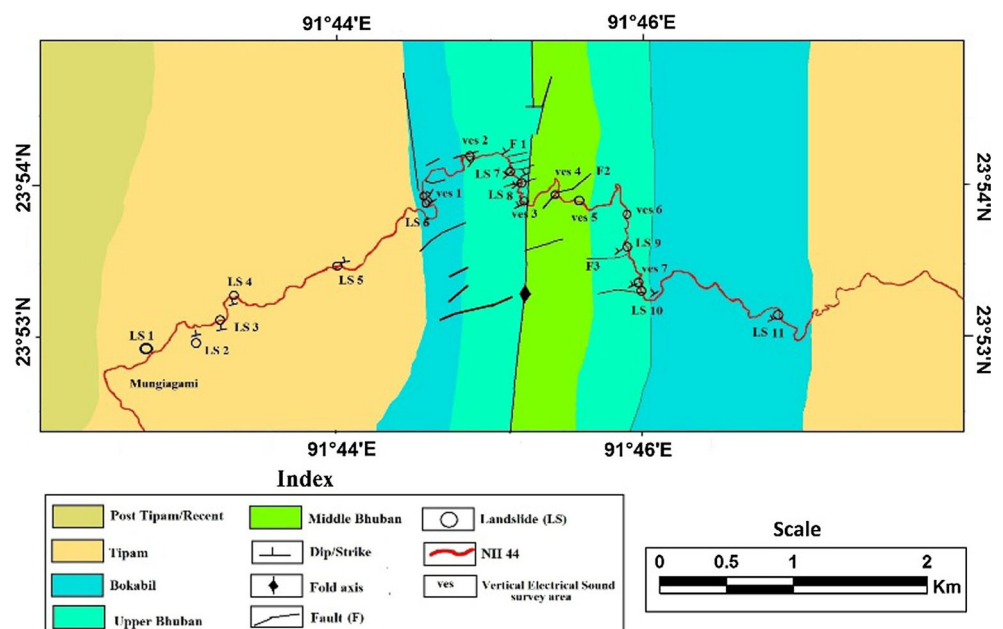
Regional geological setting

The north–south directed parallel hill ranges of Tripura fold belt are differentiated by the synclinal valley. The Atharamura Hill is comprised of Surma Group (Tertiary Period) which is characterized by alteration of sand and clay rock structure. The predominance of marine deposits in Miocene–Pleistocene age, which is immediately followed by upliftment of the landmass, creates this fold belt (Table 1). Thick deposition of fine sand in the western and eastern limb part of the Atharamura Hill belongs to Tipam Group. It is formed after the Bhuban and the Bokabil Formation of Surma Group. The fluctuation of micro tidal to meso tidal coastal environment plays a dominant role in the formation of sand to

sandy clay and clayey sand to thick clay rock structure in Surma Group. The Middle Bhuban Formation is characterized by the alteration of sand and clay rocks.

The axis of anticline portion of the hill exposed along the road is characterized by cross stratifications (dip 26°, 34°; paleo-current direction NW–SE, N–SE). The alignment of the bedding indicates two major directions from which deposition started, i.e., northwestern to southeast and north to southeast trend. The detailed dip and strike data plotted on the regional geological map indicate the inclination (dip) of the western most portions is varying 9°, 12° and 14°, respectively (Fig. 1). Maximum dip was recorded close to the fold axis, i.e., more than 45°. The regional geological map provides a clear idea about the structural

Fig. 1 The regional geological map indicates the litho-tectonic characteristic of the study area. The location of the landslide (LS) along the National Highway (NH) 44 and the survey area (VES) provide the relationship between the geological set up and the hazard scenario



pattern, lithological characteristic and moreover its relation with the landslides. The existence of the major fault can be found in the Bhuban and Bokabil Formation which is characterized by clay stone and mud stone. Thin section analysis of the sample collected from the fault zone indicates that the grain size of the rock is 218–2774.50 μm . The brittle deformation within quartz is clear in the sample. It is the indication of elastic energy release and grain boundary sliding. The grains are mostly angular to sub-angular. The Tipam Group comprised clay stone as well as sandstone. The most significant feature revealed from the regional geological map is that the landslide LS 1, LS 2, LS 3 is debris fall (sandstone), whereas LS 4 and LS 5 are earth fall (sand and clay), and the rest is rock slide. The rock slides are found mostly in the Surma Group which is dominantly clay stone and mud stone.

Study area

The Atharamura Hill is the second hill range from the west after Baramura Hill which is the part of Tripura fold belt (Fig. 2b). The present study has been conducted along National Highway (NH) 44 (11.8 miles) in the Atharamura Hill (Fig. 2). The latitudinal extension is 23°53'N–23°55'N and longitudinal extension is 92°42'E–92°48'E. Some of the prominent faults have been identified along the road (Fig. 2c). The major landslides are located close to these faults. Three major types of landslide have been identified, i.e., debris fall, earth fall and rock slide. The debris fall and earth fall are located away from the fold axis. Rock slide can be found close to the fold axis where maximum concentration of fault can be found. The Google Earth images also clearly indicate the faults and the landslide areas. The

Fig. 2 Seismic zonation map of India (a) shows that Tripura falls under high risk zone (zone V). The geological map of Tripura (b) is indicating the location of the Atharamura Hill. The location of National Highway (NH) 44, major structural feature and the landslides are plotted in the map (c)

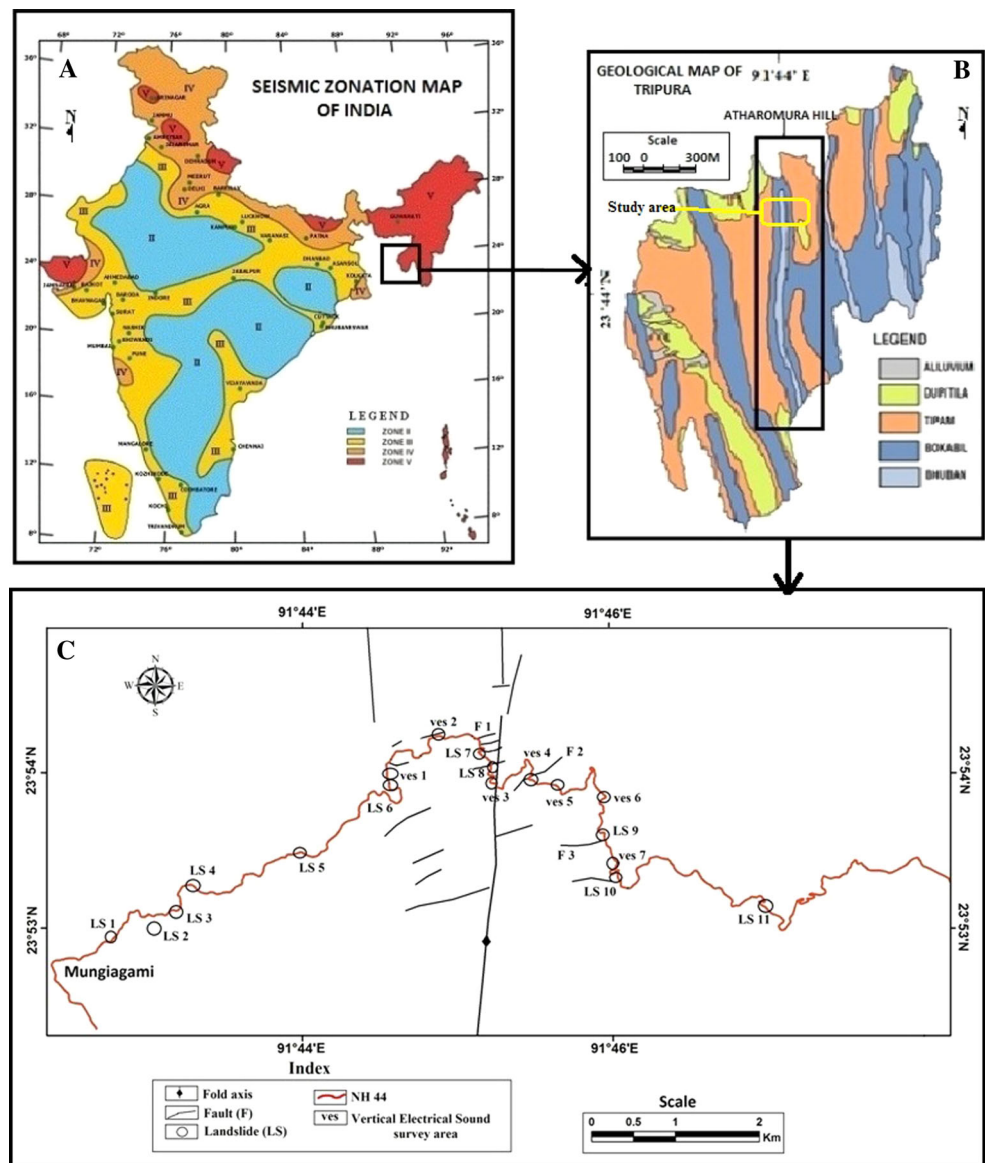
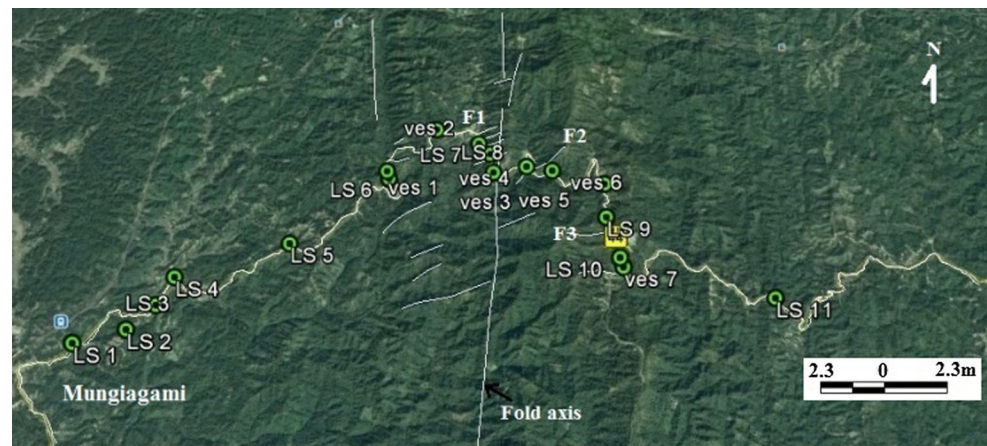


Fig. 3 Google Earth map shows the structural characteristic, landslides and the National Highway (NH) 44. The correlation between structural characteristic and landslide has been identified



LS = Landslide ves=Vertical electrical sound survey area F= Fault

axis portion of the fold is also characterized by north–south trending fault (Fig. 3). The photographs indicate the vulnerable conditions in the landslide zones which are located close to the fault F1 (Fig. 4a). The sample for preparation of a thin section was collected from the core of the fault (Fig. 4a1). The water-bearing strata are exposed along the fault. The retention wall has been constructed and water-bearing strata are channelized to prevent the landslide. The earth fall comprised a pile of sand and clay materials located in the western portion of the fold axis (Fig. 4b). The debris fall, which comprised sand materials, falls directly through vertical slope (Fig. 4c).

The schematic diagram of the three landslides has been prepared in order to study the phenomena (Fig. 5). The earth fall is associated with fault (F1), the rock beds which are sliding down along the bedding plane. The fault expedites no dip slip component; only strike slip can be identified (Fig. 5a). The earth fall is characterized by the heap of material (clay and sand) falling through vertical slope, whereas the debris fall is characterized by the sand material (Fig. 5c). The poor, lithified sandstone is clasped from the crest (upper) portion of the exposed rock bed. The slope is abundantly vertical (inclination more than 65°). The fall type of landslide (earth and debris) has been found where the dip portion of the rock bed is exposed.

Methodology

Initial field planning

The handheld global positioning system (GPS) receiver (L-1 signal) is used for locating the landslides and different faults. For collection of the data, a minimum of four precision approach (PA) conditions of L-1 signal (3D positioning) were considered for minimizing the vertical and

horizontal data error. The wide area agglomeration system (WAAS) signal was received at 6 m accuracy. The data are plotted on the base map and satellite images. The accurate data regarding the location of landslide and existing fault are the platform for understanding the research problem. During the field work, structural condition (bedding patterns and lithology), fault characteristic and recent landslide were observed carefully. Brunton compass and measuring tape were used for structural study.

Digital operation and preparation of base map

Many researchers like Thomson et al. (1990), Bolstad et al. (1998) and Abbate et al. (2006), attempted to assess the relationship among vegetation covers, geomorphic or geological characteristics by using remote sensing technique. During the recent decade, thermal remote sensing was also applied for assessing regional level seismo-tectonic activity (Tronin 2000). At the initial level of this work, a geological map prepared by GSI (Geological Survey of India), road map of Tripura and Google Earth images were consulted for field planning. Several spectral resolutions of Landsat TM, ETM+ images were used for digital operation. The Landsat image data set comprised thermal bands, which are very useful for the lineament mapping. The experiment of the spectral ranges has been done to reveal the best possible visualization of the faults. The DN (digital number) is classified (unsupervised classification) into four classes. The band combination of infrared bands like short-wave infrared or SWIR (2.08–2.35 μm), mid-wave infrared or MWIR (1.55–1.75 μm) and near infrared or NIR (0.76–0.90 μm) were prepared initially. This combination is considered as suitable for detecting lineaments. Thermal infrared band (10.40–12.50 μm) was classified in automated mode for the identification of spatial range surface thermal emission characteristics. Finally, the combination of spectral ranges

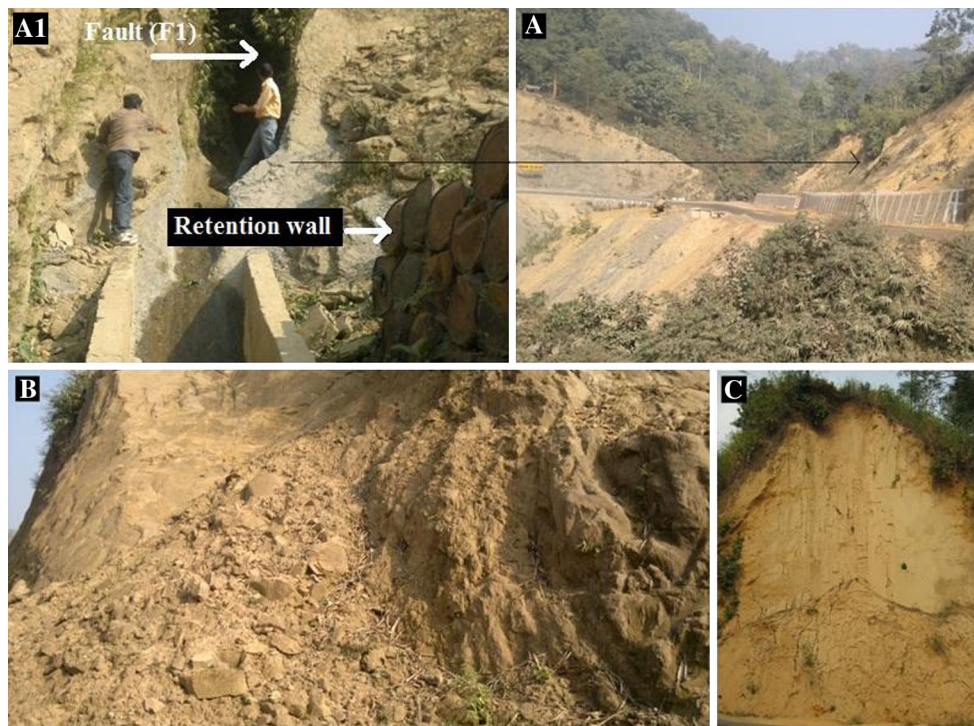


Fig. 4 Photographs show the three major landslides (debris fall, earth fall and rock slide) in the Atharamura Hill, portion of Tripura fold belt. The rock slide (**a**, **a1**) is identified close to fault (F1). The exposed water-bearing strata have been identified. The retention wall

has been constructed to protect landslide (**a1**). The earth fall (**b**) and debris fall (**c**) have been identified. The lithological composition of rock change in the slide zones (**a**, **b** and **c**)

Fig. 5 The schematic diagram of the three landslides indicates that rock slide (**a**) is associated with the existence of the fault (F1) which is sliding along the strike. The earth fall is characterized by mixing material of clay and sand (**b**). The debris fall is composed of loose sand (**c**)

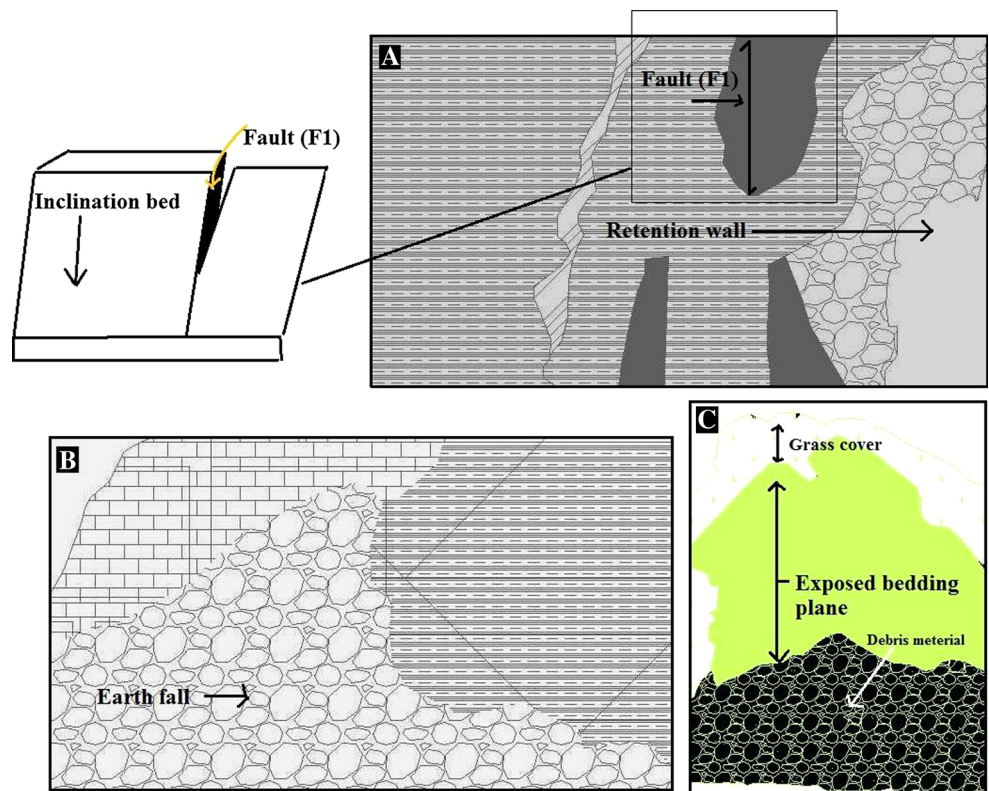
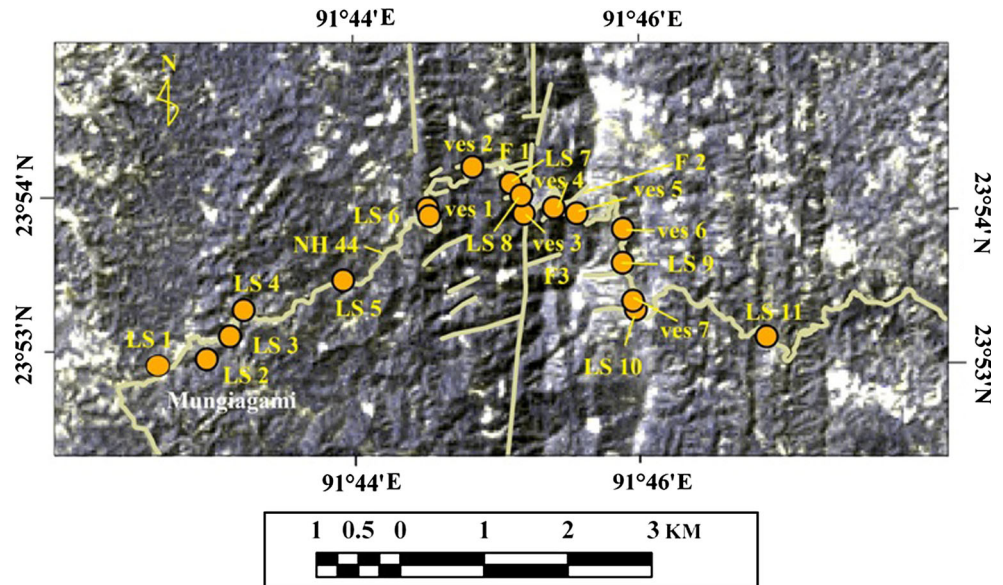


Fig. 6 The geothermal image of the study area indicated the spectral variation of different faults identified previously (Figs. 2, 3). The E–W trending faults have been identified by *dark tone* (High thermal absorption). The major faults have been plotted along NH 44, surveyed area (VES) and landslides (LS) have also been identified



was overlaid by classified thermal infrared band for detecting the lineaments (Fig. 2). The NH 44 is plotted and the landslide area is also marked in order to make comparison of different data.

Soil electrical resistivity survey

Geo-electrical survey was carried out for verifying the soil electrical resistivity characteristics of the study area. In the present study, vertical electrical sound (VES) method was adopted for assessing structural condition. Early works by Christensen (Sørensen 1996), Dahlin (1996), and Dahlin et al. (1997) strongly support the efficiency of this technique in identifying the physical characteristics of rocks. The electrical resistivity of rock depends on the pore space and the water-bearing strata. The subsurface structural characteristic can be identified without digging the soil; so, this geophysical method is very useful for educational purposes. Some authors like George et al. (2008), Akpan et al. (2009), Ding-wen et al. (2012), and Islam T Chik Z Mustafa MM Sanusi (2012) proved the efficiency of the geo-electrical method in hazard management or investigation of groundwater condition. Seven different places (VES) in the study area were selected for geo-electrical survey. Wenner's alfa configuration was adopted for VES survey and instrumental reading was taken up to 5 m depth. The instrument was calibrated carefully. Range of the instrument was fixed 10X (current, 100 volts). The resistivity was calculated by the simple formula:

$$P = 2\pi aR$$

where, $\pi = 3.1428$ (constant), $\rho =$ Resistivity of rocks in Ωm , $a =$ Spacing of electrodes, $R =$ Range of the instrument 10X (current 100 v).

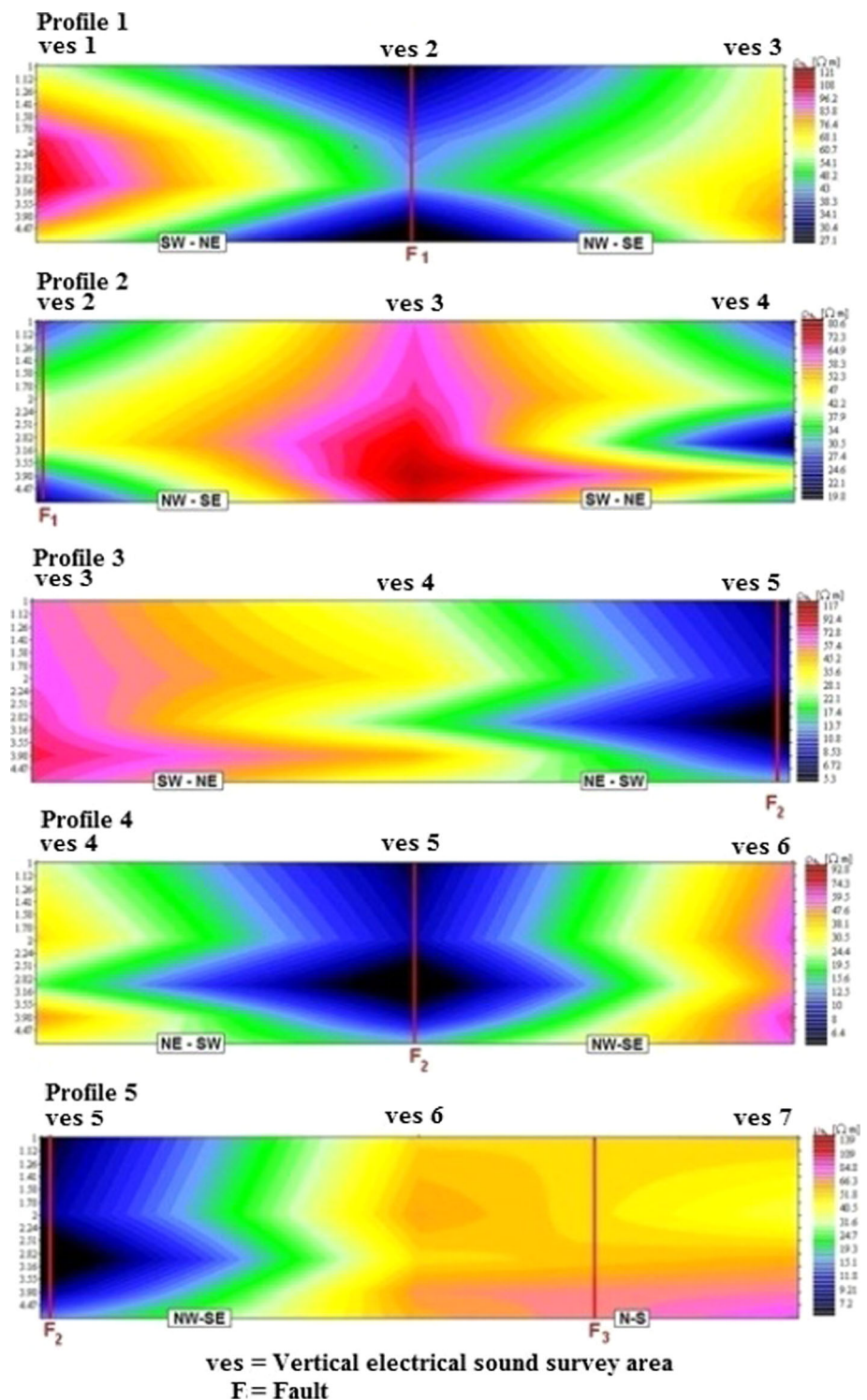
The subsurface soil electrical resistivity profile is prepared on the basis of this formula. The profile is prepared by IPI2win software. The vertical scale of all the profiles remains the same for comparing the dataset.

Results and discussions

Correlation of fault behavior and occurrence of landslide

The stress data on Atharamura Hill indicate that SH azimuth is 91° , whereas the depth is 37 km. It is located 359 km from the nearest plate boundary (CCB). The focal mechanism indicates single focal mechanism (www.world-stress-map.org). The type of magnitude is 5.4 M. Another stress field data in the Atharamura Hill indicates that SH azimuth is 48° whereas the depth is 36 km. The quality indicates C and regime TF. The $z = 37\text{ km} - P = 263\text{--}00 - T = 180\text{--}89$ from other two locations, namely RA-JEXX88#78. It is also located 369.5 km from the nearest plate boundary (CCB). It is also found to be a single focal mechanism where azimuth of S1 (P axis) 48° , Plunge of S1 (P axis) 9° , azimuth of S2 (B axis) 315° , plunge of S2 (B axis) 18° , azimuth of S3 (T axis) 164° , the plunge of S3 (T axis) 70° . The type of magnitude is 5.4 (MS). In faults identified it is possible strike slip characteristic. The displacement is observed along the strike whereas dip slide component is not much remarkable. The fault (F1) is the assemblage of three parallel faults directed clearly in an E–W direction. The plastic deformation can be well attributed. The rock samples are medium grain caring the evidences of elastic energy release. The two landslides (LS 7 and LS 8) are located along the fault (F1). The most

Fig. 7 The soil electrical resistivity profiles indicate the subsurface (5 m) structural characteristics of fault zone. The major faults (F1, F2 and F3) are identified (Fig. 6) also plotted on the profile



interesting finding is that these two landslide zones are located in the area where N–S trending faults are E–W trending faults and coincide but the landslide is following the trends of E–W faults. The landslides (rock slide) are the fault related phenomenon. The other two faults, i.e. F2 and F3, are parallel to the F1 fault. The landslide LS 9 is located close to the fault F3. The mechanism of the fault F1

and F2 and grain scale deformation of rock reveal that the activeness of the fault is accelerated by the continuous flow of exposed water-bearing strata. The sliding down of the rock bed is the result of the motion along the fault zone. The study reveals that the faults (F1, F2 and F3) might be the strike slip faults with the possibility of a very low rate of lateral movement so that major displacement cannot be

Table 2 Soil electrical resistivity data in the seven different locations along the NH 44 the Atharamura Hill indicate the shallow subsurface structure

Survey area code	Latitude	Longitude	Depth (m)	Reading (Ωm)	Resistivity (Ωm)
VES 1	23°53.951'	91°44.550'	1	0.923	57.9938
			2	0.826	103.7982
			3	0.593	111.7778
			4	0.368	92.4884
			5	0.212	66.6017
VES 2	23°54.222'	91°44.863'	1	0.417	26.2008
			2	0.311	39.0814
			3	0.229	43.1654
			4	0.116	29.1539
			5	0.07	21.9911
VES 3	23°53.921'	91°45.228'	1	0.995	62.5176
			2	0.524	65.8477
			3	0.396	74.6442
			4	0.285	81.6283
			5	0.233	73.1991
VES 4	23°53.964'	91°45.438'	1	0.411	25.8238
			2	0.294	36.9451
			3	0.102	19.2265
			4	0.191	48.0035
			5	0.093	29.2168
VES 5	23°53.928'	23°53.928'	1	0.093	5.8433
			2	0.058	7.2885
			3	0.021	3.9584
			4	0.028	7.0371
			5	0.046	14.4513
VES 6	23°53.831'	91°45.924'	1	0.154	50.3911
			2	0.085	61.8265
			3	0.262	49.3858
			4	0.264	66.3504
			5	0.187	58.7477
VES 7	23°53.311'	91°46.020'	1	0.837	52.5902
			2	0.295	37.0793
			3	0.312	58.8106
			4	0.284	71.3769
			5	0.274	86.0796

VES 1 and VES 5 are the fault zones

found but some continuous landslides have occurred as a result of the movement. But it still needs more monitoring and systematic study.

Geothermal characteristic along the fault

The geothermal characteristic of faults in the Atharamura Hill is identified (Fig. 6). The thick vegetation cover along the fault zone is the key indicator of the fault detection study.

The spectral characteristic along the faults (F1, F2 and F3) is changed due to the exposed water-bearing strata and change in vegetation cover. It is marked by dark tone because the existence of the plant moisture content along the faults absorbs spectral reflectance. It is observed in the middle portion of the Atharamura Hill along the N–S and E–W trending linear spectral signature. The DN range along the fault is >63.75 (8 bit data set). The fault lines intersecting the fold axis (N–S) and landslide zone are following particular. In some of the fold axis portion where the fault exists, the geothermal emission characteristic changes.

Analysis of near surface soil electrical resistivity characteristic

In the first profile both VES 1 and VES 3 represent moderate level of electrical resistivity characteristics up to 5 m depth (Fig. 7). At VES 1 maximum resistivity was recorded at 111.77 Ωm (3 m depth) and at the survey area of VES 3 maximum resistivity was recorded at 81.62 Ωm at the depth of 4 m (Table 2). At the VES 1 and 3 minimum electrical resistivity was observed <100 Ωm near surface at 1 m depth (57.99 Ωm and 62.51 Ωm , respectively). In this profile VES 2 is representing lowest average electrical resistivity characteristic. At this point maximum electrical resistivity was observed only at 43.16 Ωm (3 m depth). This first profile shows that the general tendency of electrical resistivity curve in this area is getting lower below 4–5 m depths. Around VES 2 the west to east extended fault (F₁) is exposed along the road between VES 1 and VES 2 which may have deteriorated the shallow soil electrical resistivity and results in some prominent slope failure like earth fall (clay stone and sandstone) and debris fall (sand stone) in this place.

The second profile is the continuation of profile 1 prepared on the basis of data collected at the areas of VES 2, VES 3 and VES 4. At VES 4 the average resistivity again recorded very low. Highest resistivity at this point is observed at 48.00 Ωm (4 m depth). Between VES 2 and VES 3 no significant slope failure has been observed. Third profile includes VES 3, VES 4 and VES 5. This profile shows the lowest soil resistivity (up to 5 m depth) of the study area. Maximum resistivity was recorded only at 14.5 Ωm (5 m depth). In this profile a remarkable elastic deformation of rock bed has been observed near VES 5 (F₂). The deformation is also evidenced in the rock micro structure of the collected samples. Between VES 4 and VES 5 (surrounding the faulted zone) a huge amount of earth/debris fall has been observed. In this place water-bearing strata have been exposed by elastic deformation. The VES 6 is characterized by comparatively higher soil resistivity than VES 5. Maximum soil resistivity was recorded at 66.35 Ωm (4 m depth). In profile 4 between

VES 4 and VES 6 some very minor slope failure has been observed particularly near F_3 . This fifth profile included VES 5, VES 6 and VES 7 in which two W–E directed faults have been observed. Near VES 5, the fault F_2 is situated and between VES 6 and VES 7 fault F_3 is situated. In this profile some debris fall is observed in the northern part of F_3 .

Conclusion

The present study shows the existence of north–south directed faults and east–west directed faults exposed along the road. Fookes et al. (1966) and Varnes (1978) considered that geological and structural settings along the slopes are the main influencing factors for mass movement development. The study reveals that most of the landslides are found surrounding west to east trending faults along the NH 44. In this study no remarkable landslide has been observed near the North–South extended faults. In some recent works Margielewski (2006) and Prager et al. (2009) have suggested tectonic setting as one of the main factors for seismic hazards. The landslide activity along the fault zone indicates the presence of active seismo-tectonism. Due to the lack of seismic observatory close to this area, it is not possible to get seismic data. However, the morphological signature like landslide indicates this possibility. In the past few years earthquake data indicate the evidences of a low magnitude earthquake in this area. For this reason a micro-seismic survey is required for understanding the regional fault mechanism. It is significant because the faults (F_1 , F_2 and F_3) extended a few kilometers only. It is also found that the impact of unscientific road-cutting and uncontrolled movement of heavily loaded vehicles may play an additional role in creating disturbance along the fault. Although the impact of the landslide is still not much destructive in the study area, there is every possibility to increase in future with the activation of faulting. Thus, from scientific point of view, more monitoring on micro-seismicity is needed for managing seismically influenced hazards in this area.

Acknowledgments Authors are grateful to Late Dr. Sudip De for tendering his innovative ideas and guidance. Authors are also thankful to Gungan Mukherjee, Susmita Paul and Shreya Bandhyopadhyay for their help and cooperation. The authors are also grateful to James W. LaMoreaux, Editor-in-Chief, Environmental Earth Sciences and the learned reviewers for providing their valuable suggestions for upgrading the manuscript.

References

- Abbate G, Maria Cavalli R, Pascucci S, Pignatti S, Poscolieri M (2006) Relations between morphological settings and vegetation covers in a medium relief landscape of Central Italy. *Ann Geophys* 49(1):153–165
- Acharyya SK (1998) Break-up of the greater Indo-Australian continent and accretion of blocks framing south and east Asia. *J Geodyn* 26:149–170
- Akpan AE, George NJ, George AM (2009) Geophysical investigation of some prominent gully erosion sites in Calabar, southeastern Nigeria and its implications to hazard prevention. *J Disaster Adv* 2(3):46–50
- Bhattacharjee S (1998) Earthquakes in northeast India Mitigation—a possible approach. In: Sharma GD (ed) Status of landslides in northeast India and Natural Disaster Management. Assam University Press, Assam, pp 77–84
- Bolstad PV, Swank W, Vose J (1998) Predicting Southern Appalachian over story vegetation with digital terrain data. *Landsc Ecol* 13:271–283
- Booth MA, Roering JJ, Perron JT (2009) Automated landslide mapping using spectral analysis and high-resolution topographic data: Puget Sound Lowland Washington and Portland Hills, Oregon. *Geomorphology* 109:132–147
- N Christensen K Sørensen 1996 Pulled array continuous electrical sounding PA-CVES, with an additional inductive source Proc SAGEEP' 96 (Symposium on the application of geophysics to engineering and environmental problems) Environmental and engineering geophysical society Wheat Ridge, USA 110
- Curry JR, Moore DG (1974) Sedimentary and tectonic processes in Bengal deep-sea fan and geosyncline. In: Burk CA, Drake CL (eds) The Geology of Continental Margins. Springer, New York, pp 617–628
- Curry JR, Emmel FJ, Moore DG, Raitt RW (1982) Structure, tectonics and geological history of the northeastern Indian Ocean. In: Nairn AEM, Stehli FG (eds.) The Ocean Basins and Margins. The Indian Ocean, Vol 6 Plenum, NY, pp 399–450
- Dahlin T (1996) 2D resistivity surveying for environmental and engineering applications. *First Break* 14:275–283
- Dahlin T, Loke MH (1997) Quasi-3D resistivity imaging—mapping of three dimensional structures using two dimensional DC resistivity techniques. In: Proc 3rd meeting environmental and engineering geophysics. Environmental and engineering geophysical society European section, Aarhus, Denmark, pp 143–146
- Dey S (2005) Conceptual models for the assessment of tertiary-quaternary geomorphic evolution of Paleo-coastal Tripura. *Ann Nat Assoc Geogr XXV(1)*:73–80
- Dey S, Sarkar P, Debbarma C (2009) Morphological signatures of fault lines in an earthquake prone zone of southern Baromura hill, north-east India: a multi sources approach for spatial data analysis. *Environ Earth Sci* 59(2):353–361
- Dey S, Sarkar P, Debbarma C, Paul S (2011a) Seismic assessment in southern Baramura hill, northeast India, considering geophysical aspects. *Environ Earth sci*. doi:10.1007/s12665-011-1249-8
- Dey S, Paul S, Debbarma C, Sarkar P (2011b) Experiment on visualizing for assessing late-Tertiary microstructural evidences of depositional changes in Gajalia fold, south Tripura. *J Geol Soc India* 77:367–376
- Ding-wen Z, Lei C, Key Song-yu (2012) Key parameters controlling electrical resistivity and strength of cement treated soils. *J Cent South Univ* 19:2991–2998. doi:10.1007/s11771-012-1368-8
- Eeckhaut MVD, Poesen J, Verstraeten G, Vanacker V, Moeyersons J, Nyssen J, Beek LPHV (2005) The effectiveness of hillshade maps and expert knowledge in mapping and old deep-seated landslides. *Geomorphology* 67:351–363
- Eeckhaut MVD, Vanwallenghem T, Poesen J, Govers G, Verstraeten G, Vandekerckhove L (2006) Prediction of landslide susceptibility using rare events logistic regression: a case-study in the Flemish Ardennes (Belgium). *Geomorphology* 76:392–410

- Falvey DA (1974) The development of continental margins in plate tectonic theory. *J Aust Pet Explor Assoc.* 14:95–106
- Fookes PG, Wilson DD (1966) The geometry of discontinuities and slope failures in Siwalik Clay. *Geotechnique* 16(4):305–320
- George NJ, Akpabio GT, Evans UF (2008) Study of failed tarred roads using earths resistivity values from local communities in Ukanafun local government area Akwa Ibom state, Nigeria. *Integr J Phys Sci* 3(1):1–5
- Guha SK, Bhattacharya U (1984) Studies on prediction of seismicity in northeast India. In: *Proceedings of World Conference on earthquake engineering, San Francisco, USA, July*, pp 21–27
- Gupta HK (1993) Patterns preceding major earthquakes in northeast India. *Curr Sci* 64:889–893
- Gupta HK, Singh VP (1982) Is Shillong region, northeast India, undergoing dilatancy stage precursory to a large earthquake? *Tectonophysics* 85:31–33
- Gupta HK, Singh HN (1986) Seismicity of northeast India region: part II: earthquake swarm precursory to moderate magnitude to great earthquakes. *J Geol Soc India* 28:367–406
- Gupta HK, Singh HN (1989) Earthquake swarm precursory to moderate magnitude to great earthquakes in northeast India region. *Tectonophysics* 167:255–298
- Islam T, Chik Z, Mustafa MM, Sanusi H (2012) Modeling of electrical resistivity and maximum dry density in soil compaction measurement. *Environ Earth Sci* 10.1007/s12665-012-1573-7
- Jaisawal K, Sinha R (2006) Probabilistic modeling of earthquake hazard in stable continental shield of the Indian Peninsula. *ISET J Earthq Technology* 43(3):49–64
- Kayal JR (1987) Microseismicity and source mechanism study: Shillong Plateau, Northeast India. *Bull Seismol Soc Am* 77(1):184–194
- Lal H, Singh NP, Tandon AK (2012) Mapping of reservoir facies within heterogeneously deposited and structurally deformed strata in Tripura frontal fold belt of Assam and Assam Arakan basin: application of sequence stratigraphy, 3D Seismic Attributes and Inversion, AAPG International Conference and Exhibition, Singapore, September 16–19, pp 23–24
- Lee TT, Lawver LA (1995) Cenozoic plate reconstruction of Southeast Asia. *Tectonophysics* 251:85–138
- Margielewski W (2006) Structural control and types of movements of rock mass in anisotropic rocks: case studies in the Polish Flysch Carpathians. *Geomorphology* 77:47–68
- McKenzie D, Sclater JG (1971) The evolution of the Indian Ocean since the late cretaceous. *R Astron Soc Geophys J* 24:437–528
- Prager C, Zangerl C, Nagler T (2009) Geological controls on slope deformations in the Koefels Rockslide area (Tyrol, Austria). *Austrian J Earth Sci* 102(2):4–19
- Sass O, Bell R, Glade T (2008) Comparison of GPR, 2D- resistivity and traditional techniques for the subsurface exploration of the Oschingen landslide, Swabian Alb (Germany). *Geomorphology* 93:89–103
- Smith AG, Hallam A (1970) The Fit of Southern Continents. *Nature* 225:139–144
- Steady S, McCloskey J, Bean CJ, Ren J (1996) Heterogeneity in a self-organized critical earthquake model. *Geophys Res Lett* 23(7):383–386
- Thomson AG, Jones C (1990) Effects of topography on radiance from upland vegetation in North Wales. *Int J Remote Sensing* 11(5):829–840
- Tronin AA (2000) Thermal IR satellite sensor data application for earthquake research in China. *Int J Remote Sensing* 21(16):3169–3177
- Varga RJ (1997) Burma. In: Moores EM, Fairbridge RW (eds) *Encyclopedia of European and Asian regional geology*. Chapman and Hall, London, pp 109–121
- Varnes DJ (1978) Slope movement, types and processes, in: *Landslides analysis and control*, edited by: Schuster, R. L. and Krizek, R. J. Transportation Research Board, national academy of sciences, Washington, D.C., Special Report 176, pp 11–33